

## Discovery of an Unmelted H-Chondrite Inclusion in an Iron Meteorite

Ignacio Casanova, Thomas Graf, Kurt Marti

The link between H chondrites and silicate inclusions in group IIE iron meteorites has long been suspected, but direct evidence for a common parentage has remained elusive. The discovery of an unmelted chondritic inclusion in the Techado iron meteorite sheds light on the genetic relation between these two groups, providing clues on the origin of chondritic materials as inclusions in iron meteorites. It is proposed that the complex IIE iron meteorite breccias formed by collisions with several different bodies, followed by deep burial of metal and silicate fragments in the asteroidal megaregolith.

Chondrites are agglomerate rocks whose elemental compositions (of nonvolatiles) closely resemble that of the sun and are accordingly referred to as undifferentiated meteorites. The most abundant are the ordinary chondrites. They are subdivided into three main groups, H, L, and LL, which are distinguished on the basis of their metallic FeNi contents, oxygen isotopic compositions, and for the equilibrated members, mineral compositions (mainly the Fe and Mg contents in olivine and low-Ca pyroxene). Igneous meteorites (achondrites, stony-irons, and irons) are believed to form by the melting and differentiation of chondritic precursors. It is difficult to apply similar taxonomic criteria to iron meteorites, which only contain minor amounts of silicate inclusions. Hence, they are usually classified on the basis of bulk Ni and siderophile trace element (for example, Ga, Ge, and Ir) contents. Some presumably originated in asteroidal cores and exhibit compositional trends that result from fractional crystallization: These are the magmatic iron meteorites (groups IIAB, IIIAB, and IVA). In contrast, the nonmagmatic classes (IAB, IIICD, and IIE) represent the metal-rich fractions of asteroidal parent bodies that did not undergo efficient core formation (1, 2).

An understanding of the genetic links between differentiated meteorites and their chondritic precursors is expected to provide important clues about the diversity and evolution of asteroidal parent bodies and the nature of heating mechanisms (for example, radioactive element decay, impact, and electromagnetic induction). Some igneous and chondritic groups have similar chemical and isotopic compositions, but no conclusive evidence exists on the link between primitive and differentiated meteorites. The IIE iron meteorites are important in this regard because several of them con-

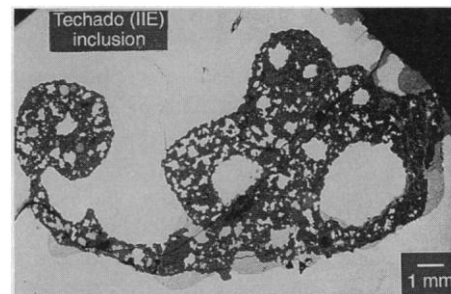
tain significant amounts of silicates whose oxygen isotopic compositions are similar to those of main-group H-chondrites and lie on the same fractionation line (3, 4). This suggests formation from an isotopically uniform reservoir and, maybe, origin in the same parent body. However, the petrologic features of these inclusions, often consisting of highly differentiated materials, are very different from those observed in ordinary chondrites.

A few IIE iron meteorites contain silicate-rich objects of a more primitive (chondrite-like) nature. Netschaëvo has angular silicate inclusions that have not undergone melting and, although obscured by recrystallization, preserve some of the original textural features (relict chondrules) of the precursor (5). However, olivine and low-Ca pyroxene compositions are outside the ranges defined by equilibrated H-group chondrites (6) and may represent a different type of chondritic material (7). Another example is Watson, which contains a large silicate body that, albeit once melted, did not suffer extensive mineral fractionation and maintains an H-chondrite-like composition (8). Here we report the discovery of a chondritic (unmelted) inclusion in Techado. The primitive nature of this silicate- and metal-rich object allows positive identification of its chondritic precursor, thus providing direct evidence of the genetic link between H-chondrites and IIE iron meteorites.

**Fig. 1.** Backscattered electron image of the silicate inclusion and part of the metal host of Techado. Silicate mineralogy (medium gray) is dominated by olivine, low-Ca pyroxene, and albitic plagioclase. Minor and accessory phases in the inclusion include whitlockite (usually at or close to metal grain boundaries), Al-rich chromite, and akaganéite, an iron oxyhydroxide product of terrestrial weathering (11). FeNi metal (white) consists of kamacite-taenite assemblages. Troilite (light gray) is concentrated at the contact between the silicates and host metal, forming lens-shaped grains with optically discontinuous striations perpendicular to the direction of maximum elongation. Dark-gray areas near the edge and around cracks are weathering products. The inclusion is surrounded by a discontinuous rim of swathing kamacite (not visible in this image) that locally reaches 1.9 mm in width.

Techado was found in 1977 (9) and was first classified as a IIE iron meteorite on the basis of the Ni, Ga, Ge, and Ir contents of the metal (10). Our study of a single section of the only recovered specimen revealed a previously unidentified, centimeter-sized silicate object. Unlike other inclusions in IIE irons (except Netschaëvo), this one is rich in metal and troilite, and the silicate fraction has not undergone appreciable melting. The irregularly shaped, elongated body extends about 1.5 cm from the edge into the main metallic mass of the meteorite (Fig. 1), forming a thick vein that locally reaches 6 mm in width. The silicate fraction displays a strongly recrystallized texture, like highly metamorphosed chondrites, with no distinguishable chondrules or glass. Olivine is the most abundant silicate mineral, displaying chemically uniform ( $\text{Fa}_{16.4}$ ; 16.4% fayalite), subhedral to anhedral crystals between 30 and 300  $\mu\text{m}$  in size. Low-Ca pyroxenes also exhibit equilibrated compositions ( $\text{En}_{83.2}\text{Fs}_{15.3}\text{Wo}_{1.6}$ ) (En, enstatite; Fs, ferrosilite; and Wo, wollastonite) and form grains with serrated boundaries that are between a few micrometers and 0.6 mm in maximum dimension. Feldspar is interstitial between olivine and pyroxene, occurring as continuous masses of up to 200  $\mu\text{m}$  in size that show a narrow compositional range between  $\text{Ab}_{79.5}\text{An}_{14.9}\text{Or}_{5.6}$  and  $\text{Ab}_{78.3}\text{An}_{15.4}\text{Or}_{6.3}$  (Ab, albite; An, anorthite; and Or, orthoclase). Troilite (FeS) contains some Ni (0.1 weight %) and is uniform in composition across the striae of the large lens-shaped grains (Fig. 1).

Modal analysis of metal and troilite carried out by point counting yielded values of 13.1 and 8.4 volume percent, respectively, consistent with those typically observed in H-chondrites (12). A detailed microscopic study in reflected light, covering about 15  $\text{cm}^2$  of the exposed surface, showed that all of the troilite in the Techado specimen is concentrated in or around the inclusion, with the exception of one rounded grain about 600  $\mu\text{m}$  in diameter found in the metal host 1.8 cm from the closest edge of the silicate body. This observation strongly



I. Casanova, Department Geoquímica-Grup Planetologia, Facultat de Geologia, Universitat de Barcelona, 08071 Barcelona, Spain.

T. Graf and K. Marti, Department of Chemistry, University of California at San Diego, La Jolla, CA 92093-0317, USA.

suggests that the estimated modal abundance of troilite is indigenous to the inclusion and that the spatial association of silicates and troilite is not purely coincidental.

Metallic FeNi in the inclusion consists of kamacite and taenite. Kamacite is uniform in composition (average weight percentages,  $\text{Fe}_{93.8}\text{Ni}_{5.8}\text{Co}_{0.4}$ ); in the inclusion, it usually contains blebs of taenite 20 to 40  $\mu\text{m}$  in diameter that are localized at or near grain boundaries. The metal host displays a well-developed Widmanstätten pattern, with no evident shock features, and taenite lamellae ranging between 200 and 600  $\mu\text{m}$  in width. Microprobe analyses across taenite grains in the inclusion and Widmanstätten lamellae show typical diffusion-controlled (M-shaped) profiles for Ni. The greatest concentrations of this element occur near the kamacite-taenite interface and are typically 45 to 47 weight %. Minimum Ni concentrations (at the centers of the zoned taenite crystals) vary with grain size. Cooling rates derived from analyses of metal in the inclusion and host are indistinguishable within the error of the method (13) and are estimated to be between 50° and 100°C per million years (Fig. 2).

Cosmic-ray exposure ages (the time between the formation of a meteoroid as a

meter-sized object and its capture by the Earth) provide important clues on collisional destruction rates, origins of meteorites, parent-body stratigraphy, and asteroid breakup events (14). Because the silicate inclusion reveals a chondritic composition, it is interesting to compare the exposure histories of Techado and other IIE meteorites with the records observed in chondrites (15). The exposure age and the size of a meteoroid are derived from the concentrations and isotopic signatures of cosmic-ray-produced noble gases. Two silicate separates from the chondritic inclusion in Techado, and a metal sample adjacent to it, were analyzed for noble gases (Table 1). The evaluation of appropriate noble gas production rates for a chondritic inclusion in an iron meteorite is more complex because of an enhanced cascade of low-energy secondary cosmic-ray particles in a matrix with high average atomic number (16). Such matrix effects are large for  $^{21}\text{Ne}$  and smaller for  $^3\text{He}$ . On the basis of the  $^3\text{He}$  data of the silicate separates, we calculate an exposure age of about 60 million years (Ma). The  $^{38}\text{Ar}$  concentration in metal yields an exposure age of about 80 or 60 Ma, depending on which production rate ( $P_{38}$  or  $P_{38}^*$ , respectively) is used. The calibration of  $P_{38}$  (17) is based on K isotopes, whereas  $P_{38}^*$  is calibrated with short-lived  $^{36}\text{Cl}$  (18). Because the  $^3\text{He}$  production rate is also based on short-lived nuclides, there is good agreement between the  $^{38}\text{Ar}$  age in metal (based on  $P_{38}^*$ ) and the  $^3\text{He}$  age of Techado silicates. The exposure ages of Techado and Colomera are similar and close to the upper end of the exposure age distribution for ordinary chondrites. However, there appears to be a small cluster of H-chondrite exposure ages in this range (19), which indicates a possible stochastic fragmentation at this time. The spallation Ne isotopic signature ( $^{22}\text{Ne}/^{21}\text{Ne} = 1.08$ ) (Table 1) can be used to deduce a small size of the Techado meteoroid (20). The nonspallogenic small  $^{36}\text{Ar}$  excesses [about  $0.5 \times 10^{-8} \text{ cm}^3 \text{ g}^{-1}$ , measured at standard temperature and pressure (STP)] in silicate separates are consistent with air Ar and may not be used to constrain trapped noble gases in bulk Techado.

The bulk K abundance in the chondritic inclusion of  $500 \pm 50$  parts per million (by weight) coupled with the average  $^{40}\text{Ar}$  concentration of the two silicate separates (renormalized to bulk composition) yield a K-Ar age of 4.6 billion years ago (Ga). A conservative lower limit of 4.2 Ga is obtained from the upper K limit and the lower  $^{40}\text{Ar}$  abundance of the silicate separates. The K-Ar age of Techado agrees well with ages obtained for the IIE iron meteorites Weekeroo Station (23) and Colomera (24) but disagrees with ages obtained for the IIE meteorites Netschaëvo (23), Kodaikanal (25), and Watson (8), which have ages of  $<4.0$  Ga (Netschaëvo has been artificially heated but shows an  $^{39}\text{Ar}$ - $^{40}\text{Ar}$  plateau). A grouping of IIE iron meteorites is also indicated in the records of exposure ages. The "old" subgroup (radiometric ages of  $>4$  Ga), which also has nearly identical oxygen isotopic signatures (Fig. 3), has longer exposure ages ( $T_e > 50$  Ma), whereas the "young" subgroup (radiometric ages of  $<4$  Ga) reveals very short exposure ages ( $T_e < 10$  Ma), which fall on or close to the major  $T_e$  peak of the H-chondrites at 7 to 8 Ma. These chronological differences imply different histories of the subgroups. It was suggested (23) that the records of gas-retention and exposure ages of the Weekeroo Station and Netschaëvo meteorites can be best explained by two parent objects.

The texture, mineralogy, and chemical and oxygen isotopic composition of the silicates in Techado attest to the unmelted, H-chondrite origin of the inclusion. The key question that must be answered by any model for the formation of IIE iron meteorites is how silicates were mixed into the metallic magma. First, it must be noted that

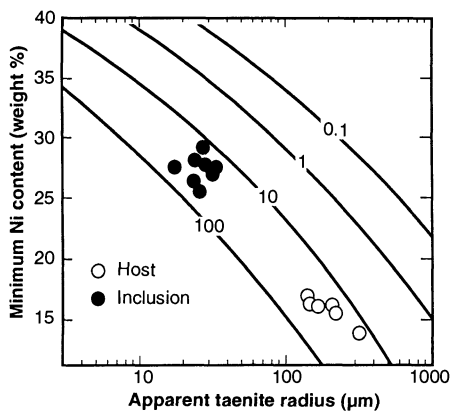


**Fig. 2.** Central Ni contents versus apparent distance to the nearest edge for taenite in host metal (Widmanstätten lamellae) and metal particles in the silicate inclusion. Metallographic cooling rate curves are from (13), for a bulk Ni content of 10 weight %. Numeric labels of the curves indicate degrees per million years.

**Table 1.** Noble gases of silicate separates (a and b) and metal samples from Techado. Typical errors are 5% for concentrations and  $<1\%$  for isotopic ratios. In the silicates,  $^3\text{He}$ ,  $^{21}\text{Ne}$ , and  $^{22}\text{Ne}$ , and in the metal,  $^4\text{He}$  and  $^{38}\text{Ar}$ , are produced entirely by cosmic rays.

Sample	Weight (mg)	Concentration ( $10^{-8} \text{ cm}^3 \text{ g}^{-1}$ at STP)					$^{22}\text{Ne}/^{21}\text{Ne}$
		$^3\text{He}$	$^4\text{He}$	$^{38}\text{Ar}$	$^{40}\text{Ar}$	$^{21}\text{Ne}$	
Silicates (a)	16.1	96	930	1.02	6400	20.9	1.084
Silicates (b)	10.5	109	989	1.54	4600	19.3	1.080
Metal	129.2	81	289	4.76	—	1.2	1.059

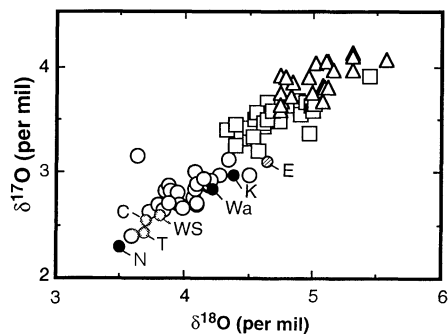


**Fig. 3.** Oxygen isotopic compositions of equilibrated ordinary chondrites (open symbols) (H, circles; L, squares; and LL, triangles) (4) and silicate inclusions in IIE iron meteorites (filled symbols). Filled circles: "young" IIE subgroup, N = Netschaëvo bulk and K = Kodaikanal pyroxene (3); Wa = Watson bulk (8). Shaded circles: "old" IIE subgroup, C = Colomera pyroxene and WS = Weekeroo Station pyroxene (3); T = Techado bulk (29). No age data are available for Elga (E); its oxygen isotopic composition (bulk) is from (3).

the nature of their silicate inclusions is quite diverse, ranging from "primitive" objects (Techado) to highly differentiated materials (Colomera). A previous model for the origin of IIE iron meteorites that argues for the mixing of silicates in a cooling metal pudding (26) is unable to explain the presence of chondritic (unmelted) objects as inclusions in large masses of (molten) metal. It has also been suggested that the silicates became incorporated into segregated, low-temperature metallic melts that were separated by shock-induced shear transport (27). This model is supported by the evidence for a "nonmagmatic" origin of IIE metal (27). However, no shock effects (such as metal veins or silicates with undulating extinction) have been detected in the silicate inclusions. Although we cannot exclude the possibility that such effects were annealed during the subsolidus history of the breccias, the absence of shock features is in conflict with the suggestion that metal and silicates in IIE iron meteorites were mixed by impact melting. Another view invokes impact mixing of silicates with a metal core from a different parent body (28). This model offers a plausible explanation for the unshocked nature of the silicates but requires a magmatic origin of the metal.

It seems necessary to call on the existence of a partially melted H-chondrite asteroid to account for the variety of silicate inclusions observed in different specimens. Some areas of this body may have preserved their primitive compositions (for example, the inclusion in Techado), and others became highly enriched in incompatible elements as a result of the fractionation of silicate magmas of minimum melt composition (represented by trydimite and potassium feldspar crystals observed in Colomera and other IIE iron meteorites). It is possible that, as a consequence of partial melting, sulfur-rich metallic liquids locally segregated and became intermingled with silicates. It is not likely, however, that such silicate objects could preserve their original metal and sulfide contents if immersed in such a metallic magma. Watson contains a good example of a silicate body that was partially melted, losing essentially all its metal and troilite, but retained a relatively undifferentiated composition (8). Therefore, mixing of the metallic liquid and partially melted silicates must have been followed by very rapid cooling of the assemblage in order to preserve the unmelted chondritic inclusion. It appears from the radiogenic ages that the "old" subgroup IIE area of the parent body was not substantially reheated by subsequent impacts. Therefore, the inferred cooling rates (Fig. 2) imply that the breccias were buried at a considerable depth in a megaregolith. Given that breccia formation

most probably took place on the surface, burial at such depths may have occurred through collisional mixing and accretion of the parental asteroids.

## REFERENCES AND NOTES

- Here, the terms "magmatic" and "nonmagmatic" are not synonymous with melted and unmelted, respectively, as commonly used in the geological nomenclature. They actually refer to different crystallization processes. However, for historical reasons, we use Wasson's (2) terminology in this paper.
- J. T. Wasson, *Meteorites: Their Record of Early Solar-System History* (Freeman, New York, 1985), p. 81.
- R. N. Clayton, T. K. Mayeda, E. Olsen, M. Prinz, *Earth Planet. Sci. Lett.* **65**, 229 (1983).
- R. N. Clayton, T. K. Mayeda, J. N. Goswami, E. J. Olsen, *Geochim. Cosmochim. Acta* **55**, 2317 (1991).
- E. Olsen and E. Jarosewich, *Science* **174**, 583 (1971).
- C. B. Gomes and K. Keil, *Brazilian Stone Meteorites* (Univ. of New Mexico Press, Albuquerque, NM, 1980), p. 31.
- R. W. Bild and J. T. Wasson, *Science* **197**, 58 (1977).
- E. Olsen *et al.*, *Meteoritics* **29**, 200 (1994).
- A. L. Graham, *ibid.* **19**, 55 (1984).
- D. J. Malvin, D. Wang, J. T. Wasson, *Geochim. Cosmochim. Acta* **48**, 785 (1984).
- V. F. Buchwald and R. S. Clarke Jr., *Am. Mineral.* **74**, 656 (1989).
- H. Craig, in *Isotopic and Cosmic Chemistry*, H. Craig, S. L. Miller, G. J. Wasserburg, Eds. (North-Holland, Amsterdam, 1964), pp. 401-451.
- J. Willis and J. I. Goldstein, *Proc. Lunar Planet. Sci. Conf. B* **12**, 1135 (1981).
- K. Marti and Th. Graf, *Annu. Rev. Earth Planet. Sci.* **20**, 221 (1992), and references therein.
- L. Schultz and H. Kruse, *Meteoritics* **24**, 155 (1989).
- J. Masarik and R. C. Reedy, *Geochim. Cosmochim. Acta* **58**, 5307 (1994).
- B. Lavielle and K. Marti, in preparation.
- F. Begemann, H. W. Weber, E. Vilcsek, H. Hintenberger, *Geochim. Cosmochim. Acta* **40**, 353 (1976).
- Th. Graf and K. Marti, in preparation.
- In the silicate samples, a correction of the  $^{22}\text{Ne}/^{21}\text{Ne}$  ratio for matrix effects is obtained by adjusting this shielding indicator to yield a value for the  $^{21}\text{Ne}$  exposure age of 60 Ma. The resulting value is  $^{22}\text{Ne}/^{21}\text{Ne} = 1.14$  for an H-chondritic matrix and may be compared with a predicted matrix-corrected value of  $>1.14$  (16). On the basis of model calculations (21), this  $^{22}\text{Ne}/^{21}\text{Ne}$  ratio restricts the shielding depth of the silicate samples to about 10 cm. Furthermore, iron meteorites with  $^4\text{He}/^{21}\text{Ne} < 250$  were inferred to have preatmospheric radii of  $<50$  cm (22).
- Th. Graf, H. Baur, P. Signer, *Geochim. Cosmochim. Acta* **54**, 2521 (1990).
- H. Voshage, *Earth Planet. Sci. Lett.* **71**, 181 (1984).
- S. Niemeyer, *Geochim. Cosmochim. Acta* **44**, 33 (1980).
- H. G. Sanz, D. S. Burnett, G. J. Wasserburg, *ibid.* **34**, 1227 (1970).
- D. S. Burnett and G. J. Wasserburg, *Earth Planet. Sci. Lett.* **2**, 137 (1967).
- G. J. Wasserburg, H. G. Sanz, A. E. Bence, *Science* **161**, 684 (1968).
- J. T. Wasson and J. Wang, *Geochim. Cosmochim. Acta* **50**, 725 (1986).
- M. Prinz, C. Nehru, J. Delaney, M. Weisberg, E. Olsen, *Lunar Planet. Sci.* **XIV**, 618 (1983).
- Techado oxygen isotopic composition:  $\delta^{18}\text{O} = 3.69$  per mil and  $\delta^{17}\text{O} = 2.43$  per mil (R. N. Clayton, unpublished data).
- We thank A. J. Brearley (Institute of Meteoritics, University of New Mexico) for providing the Techado specimen, K. V. Ponganis for assistance with noble gas measurements, R. N. Clayton for oxygen isotope analyses, J. Weinstein for photographic work, B. Strack for technical assistance with the scanning electron microscope, and T. J. McCoy for motivation and helpful comments. J. T. Wasson and an anonymous reviewer provided constructive criticism on the original manuscript. This work was partially funded by National Aeronautics and Space Administration grant NAGW 3428.

18 October 1994; accepted 27 February 1995

## DNA Solution of Hard Computational Problems

Richard J. Lipton

DNA experiments are proposed to solve the famous "SAT" problem of computer science. This is a special case of a more general method that can solve NP-complete problems. The advantage of these results is the huge parallelism inherent in DNA-based computing. It has the potential to yield vast speedups over conventional electronic-based computers for such search problems.

In a recent breakthrough, Adleman (1) showed how to use biological experiments to solve instances of the Hamiltonian path problem (HPP): Given a set of "cities" and directed paths between them, find a directed tour that starts at a given city, ends at a given city, and visits every other city exactly once. This problem is known to be NP-complete (2); that is, all NP problems can be efficiently reduced to it. A computational problem is in NP provided it can be formulated as a "search" problem. Further, a problem is NP-complete provided that if it

has an efficient solution, then so do all problems in NP. One of the major achievements of computer science in the last two decades is the understanding that many important computational search problems are not only in NP but are NP-complete. Another major achievement is the growing evidence that no general efficient solution exists for any NP-complete problem.

Thus, Adleman's result that HPP can be solved by a DNA-based biological experiment is exciting. However, it does not mean that all instances of NP problems can be solved in a feasible way. Adleman solved the HPP with brute force: He designed a biological system that "tries" all possible

Princeton University, Princeton, NJ 08540, USA. E-mail: rjl@princeton.edu